

RESEARCH

Open Access



Durability of Japanese-earth cob walls subjected to accelerated rain simulation

Emily K. Reynolds¹ and Makoto Muramoto^{2*}

Abstract

Earthen materials are increasingly being recognized in architecture for their low embodied energy, recyclability, and hygrothermal properties. However, the common use of manufactured stabilizers, while enhancing weathering resistance, compromises these merits. Japan, known for its typhoons, has used unstabilized earth in construction for centuries, suggesting the viability of this construction material. While architecture around the world attests to its resilience, in-depth research into unstabilized earthen material is limited. This study examines unstabilized earth durability through 90-min accelerated rain simulation tests, totaling over 6500 mm of “rain” exposure on each of twelve test surfaces (eight representing rural Japanese cob-ball construction and four, monolithic cob walls). Surface changes were monitored by 3D scans performed at seven intervals. The test walls were built using two common materials in Japanese earthen wall craft, sourced from the areas of Kashiba and Fukakusa. It was clear from 3D-scan analysis that the base-layer material, Kashiba, is remarkably resistant to weathering. The four monolithic Kashiba test surfaces, constructed on four different foundation types, respectively eroded just 1 mm, 2.6 mm, 3.8 mm, and 3.9 mm. These results corroborate traditional building practices. Thus, our study also underscores the value of incorporating knowledge from vernacular earthen architecture professionals in expediting academic research. Additionally, our results suggest the potential of hose-showerhead tool use for research, and for on-site testing of earthen material erosion levels for material adequacy.

Keywords Earthen construction, Unstabilized, 3D scanning, Vernacular knowledge, Hose test

Introduction

Earth-based construction (EBC) has gained significant academic attention due to growing concerns about the climate crisis and the environmental impact of conventional industrial materials. Historically, EBC played a chief role in architecture worldwide. It continues to offer unique advantages, including reduced carbon emissions, recyclability, vapor permeability, hygrothermal regulation, and long-term repairability [1–4].

The trend against earth as a building material has resulted in multiple interconnected consequences hindering its return to common use [5]. Even in research, reviews of earthen materials consistently reveal a bias against those unaccompanied by cement or lime stabilizers [2, 4, 6–8] particularly regarding durability (resistance to water). Yet manufactured stabilizers are known to compromise the benefits of EBC listed above [1, 7, 9]. Literature reveals two issues contributing to this dilemma; one, the inadequacy of existing durability tests and two, the lack of consistent methodology in testing earthen material durability.

Concerning the first issue, the early development of accepted testing methods was specifically designed for cement-stabilized earth [8]. While effective for such examinations, Beckett et al. [7] observe that unstabilized earthen materials fail common immersion, drip,

*Correspondence:

Makoto Muramoto
muramoto@kit.ac.jp

¹ Graduate School of Science and Technology, Doctoral Program of Architecture, Kyoto Institute of Technology, Matsugasaki, Sakyo-ku, Kyoto 606-8585, Japan

² Faculty of Design and Architecture, Kyoto Institute of Technology, Matsugasaki, Sakyo-ku, Kyoto 606-8585, Japan



© The Author(s) 2024. **Open Access** This article is licensed under a Creative Commons Attribution 4.0 International License, which permits use, sharing, adaptation, distribution and reproduction in any medium or format, as long as you give appropriate credit to the original author(s) and the source, provide a link to the Creative Commons licence, and indicate if changes were made. The images or other third party material in this article are included in the article's Creative Commons licence, unless indicated otherwise in a credit line to the material. If material is not included in the article's Creative Commons licence and your intended use is not permitted by statutory regulation or exceeds the permitted use, you will need to obtain permission directly from the copyright holder. To view a copy of this licence, visit <http://creativecommons.org/licenses/by/4.0/>. The Creative Commons Public Domain Dedication waiver (<http://creativecommons.org/publicdomain/zero/1.0/>) applies to the data made available in this article, unless otherwise stated in a credit line to the data.

and accelerated erosion laboratory tests. Even in cases where unstabilized earth specimens do not fail laboratory tests, measurements do not resemble those of tests performed in a natural setting, making the laboratory tests inadequate [10–12]. The second issue of inconsistencies in methodology and parameters has led to calls for universally applicable tests [2, 7]. To address this decades-long challenge, Beckett & Faria [13] recently proposed a generic accelerated erosion testing method, with further efforts required for its realization.

Equally challenging, Losini et al. [2], and others, advise researchers to conduct complete analyses of earth samples, including characterization of clay minerals. The cost of such profiles, however, can deter research advances. Danso et al. [4] note that conducted tests depend on available testing equipment. Medvey and Dobszay [8] emphasize the need for thorough investigation into the erosion mechanisms and durability of unstabilized earthen building materials. The current study addresses this under-investigated topic.

We conducted durability tests on two earth building materials from the central western (Kansai) region of Japan, which are commonly sourced by practitioners; one for base-layers and one for plaster application. Three-dimensional scanner imagery enabled detailed analysis of deterioration for twelve unstabilized earthen test wall surfaces exposed to 90 min of accelerated rain simulation, with each wall surface subjected to over 6500 mm of water. Among the twelve test surfaces, four modeled monolithic cob wall construction, a heritage process described in detail by Hamard et al. [14]. The remaining eight modeled simple cob-ball walls found in farm shed construction in rural Japan [15–17]. Research of these sheds suggests that foundation types may influence the degree of deterioration of earthen walls [15]. Including this hypothesis in the current study necessitated procuring and testing two types of material to examine the results for four foundation types (small stones, large stones, concrete, and concrete with periodic vertical channels).

Few examples of earthen wall durability research using rain simulation have been documented. Arrigoni et al. [9] and Hall [18] employed climatic simulation testing chambers for rammed earth (RE). Ogunye and Bousabaine [19] developed a durability test rig for earthen blocks, positioning a water source two meters above the ground. Luo et al. [20] conducted durability tests on RE by sourcing water from a height of twelve meters. Richards et al. [10] used a portable device mimicking wind driven rain, etc. for erosion tests on RE in the field. Hart et al. [21] used a portable rain simulator positioned three meters above adobe brick test wall specimens to measure erosion caused by simulated rain. For this study, we

also chose to position our water source three meters above the test wall target level, as detailed in the Methods section. While long-term outdoor studies such as those performed by Umubyeyi et al. [22] and Bui et al. [23] are ideal for reliable measurements of real-time deterioration, accelerated rain simulation can provide useful data to understand in-situ earthen wall deterioration due to the dynamic, continuous impact of water.

This study employs 3D scanning for measurements, a less common approach. Similar technologies have been used in durability studies, such as high-performance laser scanning [10], LiDAR scanning [21], and stereo-photogrammetry [23]. Scanning allows measurements at numerous points, offering detailed insights into wall surface deterioration.

Our research also emphasizes Japan's local vernacular earth building methods, a field seldom explored in published studies. Vernacular practices, exemplified by Millogo et al. [24] in Burkina Faso, impact strength and durability. Together with cultures of maintenance, we find lasting EBC throughout the world. Examples include the 900-year-old Taos Pueblo in a mountainous desert region of the USA, and—challenging misconceptions about EBC durability in wetter regions—400-year-old Himeji Castle in typhoon-prone Japan. This is not only a testament to expert knowledge and periodic “aftercare,” but also underscores the reparability of earthen materials. To our knowledge, the quantification of vernacular earth building methodology has not yet become an established field of research. However, practitioner expertise could be a vital component in academic research to expedite the use of dependable, environmentally gentle earthen building materials.

Accelerated rain simulation test method

Six double-sided earthen test walls were built on mobile platforms, providing twelve unique wall surface conditions for testing durability using accelerated rain simulation. Two of the six were built as monolithic cob, a process which involves stacking and blending clods of plastic-state earth mixed with fibers to build a monolithic wall, without the use of a form [14]. Four were of cob-ball construction, a style found in rural Japanese farm sheds, with one side left as-is and one side with a rendered finish. “Cob-ball walls” is deemed the most appropriate English term for this building style because they also employ plastic-state earth without a form for construction. Here, individual balls of plastic-state earth, with aggregates and short straw, are stacked and often covered with earthen render [15–17].

For optimum accuracy in the analysis of all twelve surfaces, 3D scans were conducted before the rain simulation, after each testing step, and once the walls had dried

at ambient temperature. The 3D scans allowed for tenth-of-a-millimeter-level deterioration measurements.

Test walls

Platforms were designed to be robust yet movable by a single person. Refer to Fig. 1 for the specifications of the test wall constants.

The earthen wall materials evaluated in this study were selected for their easy accessibility. They were sourced from two different locations: Kashiba in Nara Prefecture and Fukakusa in Kyoto Prefecture. Both materials are commonly used by professional earthen wall builders in these respective regions.

- Kashiba-sourced earth (heretofore Kashiba earth) is a sandy silt loam, commonly used as the main ingredient for base layer application over a bamboo lattice substrate. This earth is a mixture of two earths, one sourced from a former rice field and another salvaged from demolished structures. The base-layer material from demolished structures is known to retain value and is sought after for reuse in this manner. This mixed material was delivered to the testing site. It was moist, dark in color, dense, and sticky upon arrival.
- Fukakusa-sourced earth (heretofore Fukakusa earth) is a sandy loam, commonly used as the main ingredient applied as a plaster over a base layer. This serves as a flattening layer and comprises a substrate for thin finishes, such as those of the 2 mm-thick lime finish of Himeji Castle. This material was sourced directly from a mountain quarry, scooped from a pile

by an excavator and filtered through a 24 mm screen into the truck bed. It was mostly dry and yellow–red in color.

Table 1 shows the particle distribution analysis of each material.

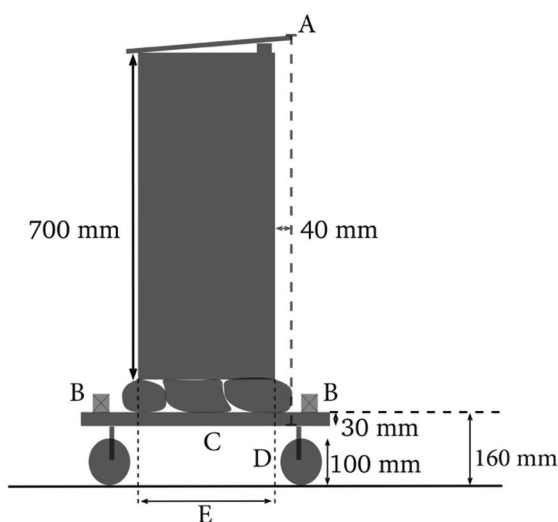
The two monolithic cob walls were constructed using earth sourced exclusively from Kashiba. Of the four cob-ball walls, two were built from Kashiba earth, while the remaining two were built from Fukakusa earth. These six walls provided twelve testing surfaces; the four cob-ball walls provided eight testing surfaces, and the two monolithic walls provided four. Each of the four cob-ball walls had one side rendered using the same material as their substrate cob balls. The other side remained unrendered, with the cob balls exposed.

Kashiba cob balls and Fukakusa cob balls were made using the same ratio of earth to rice straw, which was cut to approximately 100 mm in length; 60 L of earth to 500 g of straw. Water was added as needed, until an appropriate consistency was achieved. Table 2 lists moisture content

Table 1 Earthen Material Particle Distribution by Source

Particle Distribution (%)*	Kashiba earth	Fukakusa earth [25]
Stones (> 75 mm)	0	0
Pebbles (2–75 mm)	9.5	2.6 (none over 19 mm)
Sand* (0.075–2 mm)	46.7	53.2
Silt* (0.005–0.075 mm)	29.7	24.5
Clay* (< 0.005 mm)	14.1	19.7

*Particle distribution parameters are defined by Japan Geotechnical Society Standards



- A: 12 mm thick plywood board to provide small overhang for test wall.
- B: 40 mm x 40 mm blocks screwed onto the platform to provide an origin point in scan results to create three-dimensional images for analysis along x-y-z axis.
- C: 30 mm thick plywood board platform wrapped with heavy duty tarps and secured with water-proof tape.
- D: 100 mm diameter rubber swivel caster wheels with brake.
- E: Width of wall between testing surfaces: 330 mm for all stone foundations; 450 mm for concrete

Fig. 1 Test wall constants. All walls are hollow in the middle, like a chimney, to make the mobile platform lighter and easier to move

Table 2 Moisture Content of Materials

	Moisture content at mixing (%)	Moisture content at implementation (%)
Kashiba cob-ball	23.38	21.13
Fukakusa cob-ball	18.76	16.09
Kashiba render	22.49	Implemented immediately after mixing
Fukakusa render	21.83	
Kashiba monolithic	20.89	

of materials at mixing and at implementation measured by A&D’s MX-50 moisture analyzer [26]

Each earth was initially moistened by adding sufficient water and then evenly dispersing it with a hand-held hoe, resulting in a pliable consistency. Straw was added and mixed in. Then, slightly more water was added as needed for even straw dispersion. The pliability of the mix was such that balls could easily be formed by hand. Ball size averaged 10 to 14 cm in diameter. Undergraduate students assisted in the construction of all cob-ball walls, as this allowed for variations in ball density and size. This is imitative of in-situ conditions, where family members and neighbors participated in cob-ball shed construction [15]. After being formed, the balls were laid on the ground until they reached an optimum stage of pliable dryness—stackable, meaning they stick to one another without deforming under the weight of the next ball on top. This brief drying process was suggested by the work of Hatanaka et al. [27], who were advised by local earth-building professionals.

Rendering for cob-ball surfaces was created by adding water to exactly the same material as was used for the cob balls (Fukakusa render for Fukakusa balls, and Kashiba render for Kashiba balls). Water was added to

the material until it reached sufficient wet plasticity, suitable for rendering over the ball surface using a hawk and trowel. Rendering was performed after the cob ball wall had dried at ambient temperature. The cob balls were dampened slightly before rendering for better adhesion. Renders varied in thickness due to the undulation between balls, with approximately 5 mm of material over ball apices. All wall rendering was executed by the first author of this paper.

For monolithic wall construction, an additional 800 g of rice straw, cut in approximately 300 mm lengths, was added to the Kashiba-plus-straw mix described above. Mixing was performed using a tarp and foot pressure to flip and stir the material, adhering to methods described in the literature [28]. The pliable material was stacked immediately after mixing, with each layer reaching roughly 150 mm in height per day of application. The construction of the monolithic cob walls was undertaken solely by the first author (Fig. 2C).

The acronyms corresponding to each unique test wall surface are abbreviated and ordered throughout this article, as follows:

1. Material source location (K=Kashiba; F=Fukakusa)
2. Construction style (B=balls; R=rendered; M=monolithic) as in Fig. 3
3. Foundation type (S=small stones; L=large stones; C=concrete; Cc=concrete with periodic vertical channels) as in Fig. 4

Throughout this paper, walls are referred to as series:

- B-series refers to test walls made of cob balls.
- R-series refers to test walls made of cob balls and then rendered.

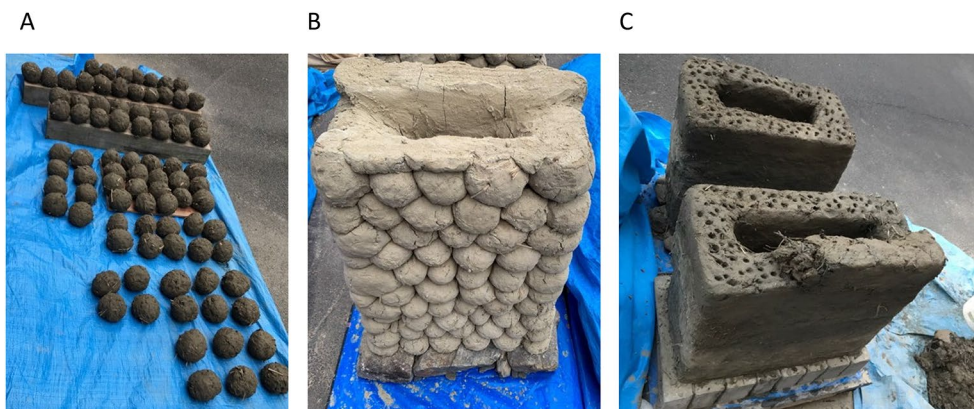


Fig. 2 Building the test walls. A: Cob balls drying before implementation. B: Cob-ball wall completed. C: Monolithic cob wall in process of implementation, material mix on right

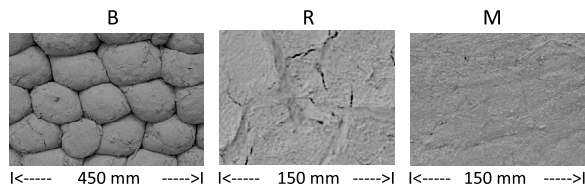


Fig. 3 Construction styles. Left to right: B (ball surface); R (rendered surface); M (monolithic)

- M-series refers to test walls made of **monolithic cob**.
- B-, R-, and M-series each comprise of four test surfaces, totaling twelve.

Table 3 provides characteristics and acronyms of each tested surface.

Testing room

Due to the substantial amount of water (1260 L per 90-min test) required for the accelerated rain simulation, an outdoor location was necessary for conducting the tests. To mitigate the impact of even slight winds, which could divert the water from its intended trajectory, a protective structure was constructed. Figure 5A shows this scaffolding-pipe structure covered by commercial-grade heavy-duty tarps.

The size of the structure was determined by the need for easy maneuverability of the test platforms and sufficient height for the pressurized water to fall three meters. It was also essential to provide a sheltered area for the scanning equipment during tests to prevent water exposure.

The testing room setup is depicted in Fig. 5B. To accommodate fluctuations in the water pressure at the delivery setting, the water delivery device output angle was inclined toward the ground at approximately 20° from horizontal. Walls were positioned and adjusted to ensure that water primarily fell on the central lower portion. The impact angle was approximately 23° for all dispersion types. This angle aligns with the 15–30° range identified by Luo et al. [20] as most conducive to erosion in rainfall simulations.

A thermo-hygrometer collected temperature and humidity data during the construction and testing period, which spanned from mid-June 2021 through the first week of November 2021. The average temperature during that time was 19.6°C with a standard deviation of 6.1 °C. Average relative humidity was 69.9%, with a standard deviation of 12.4%.

Accelerated rain simulation

The rain simulation room was specifically designed to facilitate the fall of pressurized water from a height of three meters, the height determined sufficient by Hart et al. [21] and Nielsen et al. [29].

As rain in the natural environment falls in a variety of intensities, three pressurized water delivery settings were utilized to mimic accelerated rainfall. Water setting specifications are provided in Table 4. While there is no universal agreement on the classification of rainfall intensity, “heavy rain” is generally characterized as exceeding 8 mm per hour. In this experiment, all three water delivery systems significantly exceeded this threshold.

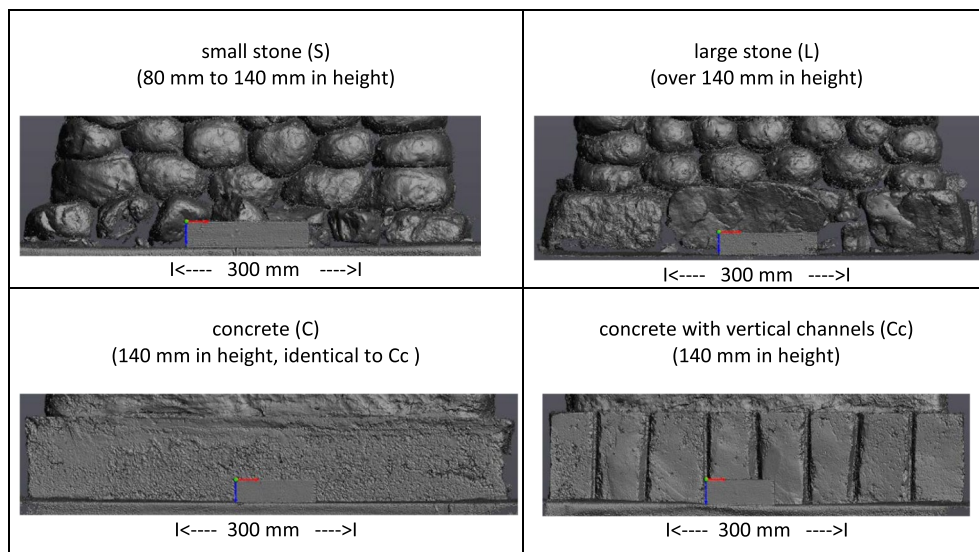


Fig. 4 Scanned images of foundation types. Note the green scanning reference point in each photo

Table 3 Test Wall Construction Type with Acronyms

	SIDE A Features/ Acronym	SIDE B Features/ Acronym	Dimensions (mm, <i>W x L x H</i>)
Cob-ball walls			
Kashiba earth; Cob balls; Large stone foundation	Cob balls KBL	Rendered over cob balls KRL	330 × 630 × 700
Fukakusa earth; Cob balls; Large stone foundation	Cob balls FBL	Rendered over cob balls FRL	330 × 630 × 700
Kashiba earth; Cob balls; Small stone foundation	Cob balls KBS	Rendered over cob balls KRS	330 × 630 × 700
Fukakusa earth; Cob balls; Small stone foundation	Cob balls FBS	Rendered over cob balls FRS	330 × 630 × 700
Monolithic cob walls			
Kashiba earth Monolithic cob; Small stone foundation	Monolithic wall, Foundation of five small stones KMS1	Monolithic wall, Foundation of six small stones KMS2	330 × 630 × 700
Kashiba earth Monolithic cob; Concrete foundation	Monolithic wall, solid concrete foundation KMC	Monolithic wall, vertical channels cut every 100 mm in the foundation KMcC	450 × 700 × 700

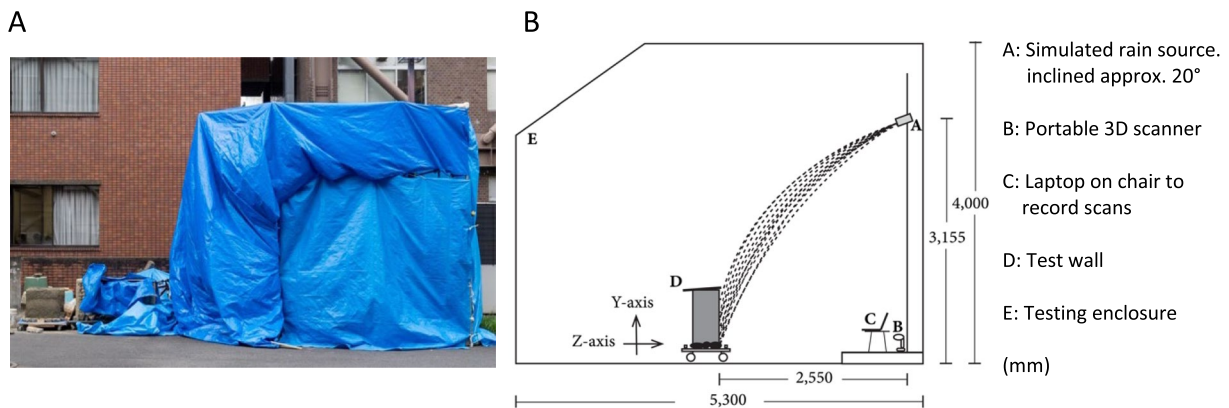


Fig. 5 Weather protective structure for performing tests. **A** As seen from the exterior. The heavy-duty tarp ensured even the slightest winds would not divert the directionality of water delivery. **B** Cross-sectional interior view of accelerated rain simulation structure

Table 4 Three Water Delivery Settings

Delivery type	Average liters per minute	Average millimeters per hour
Perforated Pipe	14	6114
Central Shower	4.7	1524
Lateral Diffusion	3.3	270

Figure 6 depicts an 18 mm diameter PVC pipe manually perforated by drilling 49 holes spaced at 8 mm intervals using a 1.5 mm drill bit, and a garden hose shower head with a 7-pattern watering nozzle (SSN-1 manufactured by Sefuti 3) which provided the central shower and lateral diffusion patterns.

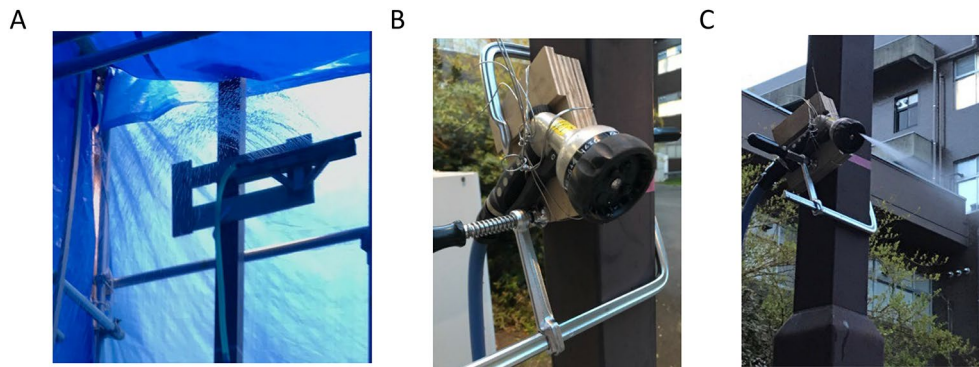


Fig. 6 Water delivery devices. **A** Perforated pipe, mounted to a frame for stability. **B** Showerhead rigged to ensure steadiness. **C** Showerhead setting on “lateral diffusion.”

A 90-min test subjected each wall surface to 6562.5 mm of simulated “precipitation.” Kyoto city receives an average annual rainfall of 1677 mm [30]. Although our simulation lacks elements such as wind force and varying water directionality, it can be inferred that our test walls sustained a nearly four-year equivalent of local rainfall within this short duration.

Testing protocol and data acquisition

The 90-min rainfall simulation of each test wall surface consisted of five successive cycles of accelerated rainfall delivery. We employed the Creaform Go!SCAN 3D 50 G2 white light portable scanning device [31]. This device performs scans in 0.500 mm resolution with up to 0.100 mm accuracy. Scans to acquire erosion data were performed before the tests, after each of the five cycles of rain simulation, and again once the surfaces were fully dried at an ambient temperature. To optimize the device’s scanning capability, we applied reflective round target stickers across the surface of the test wall prior to each scan.

Table 5 details the testing process for each of the twelve wall surfaces, outlining the sequential steps of the rain simulation and scanning procedures.

Data analysis

Data was analyzed using two software programs. In total, 84 scans (seven for each of the twelve wall surfaces) yielded a substantial dataset for comprehensive analysis.

First, the VX Model function of the software program VXelements (v.10.0.4 10726) [32] was employed to save all scanned 3D meshes at a 0.500-mm resolution. These were then exported to a GOM Inspect software program (2019 v.2.0.1) [33].

Next, in the GOM Inspect program, inspection origin points for every test wall surface were established by utilizing the X-Y-Z planes of the reference block attached to each wall surface platform.

Table 5 Accelerated Rainfall Simulation Protocol: Scanning and Duration

Step	Process	Duration (minutes)
1	3D scan of original test wall surface	
2	Perforated pipe rain simulation delivery	15
3	3D scan	29 (average)
4	Central shower rain simulation delivery	15
5	3D scan	28.5 (average)
6	Perforated pipe rain simulation delivery	30
7	3D scan	31 (average)
8	Lateral diffusion rain simulation delivery	15
9	3D scan	31.5 (average)
10	Perforated pipe rain simulation delivery	15
11	3D scan	
12	3D scan after the surface was dry at ambient temperature	

Subsequently, the meshes with set origin points were re-imported back into the VX Model software in 12 groups of seven, corresponding to the 12 different test wall surfaces. For each surface, the initial pre-test scan from Step 1 (Table 5) was sequentially combined with the remaining six scans, resulting in six combined meshes:

- Combined mesh 1: Pre-test + after 15 min water exposure (Step 3).
- Combined mesh 2: Pre-test + after 30 min water exposure (Step 5).
- Combined mesh 3: Pre-test + after 60 min water exposure (Step 7).
- Combined mesh 4: Pre-test + after 75 min water exposure (Step 9).
- Combined mesh 5: Pre-test + after 90 min water exposure (Step 11).
- Combined mesh 6: Pre-test + post-test (dry stage, Step 12).

Each combined mesh was then exported back to GOM Inspect where the image details could be viewed in 1/10 mm intervals. The subsequent analysis is described below in "Obtaining measurements" section. This enabled us to observe the progress of deterioration for each wall surface.

The scan results yielded images along the X, Y, and Z axes. The X-axis represents the horizontal plane of the test wall surface, the Y-axis, the vertical plane of the test wall surface and the Z-axis represents the results along the "depth" of the test wall surface. The X and Y axes were utilized to identify the most suitable analysis points. Subsequently, the Z-axis of the combined meshes provided deterioration values following each round of accelerated rain delivery and after the test walls dried.

Obtaining measurements

Water delivery devices were strategically positioned to concentrate the most intense rainfall at the lower 250 mm of the central area of each test wall surface. This choice stems from our observations that the most erosion-prone area of an earthen wall is at the base [15]. Additionally, research shows that gravity tends to concentrate moisture at the bottom portion of the walls, leading to more damage in that area [3, 34]. Capillary rise, the upward movement of water within porous materials, also contributes to the vulnerability of the base portion of earthen architecture [35, 36]. Consequently, our analysis was concentrated on a central 300 mm section of the X-axis from the foundation to the height of 250 mm along the Y-axis for each test wall. By examining the combined meshes at selected locations, we were able to measure deterioration along the Y–Z plane.

For the R-series walls, Fig. 7 shows our analysis of points along horizontal lines at 50 mm intervals, covering the range from the lowest measurable point to a height of 250 mm on the wall. Each of these six horizontal observation lines was assessed across the central 300 mm section at intervals of 50 mm. These measured values were then averaged to determine deterioration at each of the six selected heights of the wall. This analysis was consistently performed at identical locations across all six combined meshes for each wall in this series, providing insights into their progressive deterioration.

The M-series walls were subjected to an approach similar to that of the R-series walls, but with closer scrutiny due to the subtle nature of the observed deterioration. In addition to the six horizontal lines described previously, Fig. 8 shows four additional lines of measurement taken from the lowest 40 mm in 10 mm intervals.

The B-series wall surfaces exhibit significant undulation and therefore required a different analytical approach, shown in Fig. 9. Rather than analyzing points at specified intervals as with the R- and M-series walls, we focused our analysis on individual cob balls within the central 300 mm section at the bottom 250 mm section of the test walls. The surface apex of each cob ball was identified from the pre-experiment scans, and these locations were used as reference points for analysis. For each combined mesh, the deterioration of cob balls at their respective surface apexes was examined in the Y–Z plane. To facilitate comparison with the analysis of R- and M-series walls, we considered cob balls belonging to the same stacked layer to be in the same line. The deterioration measurements were averaged within each line.

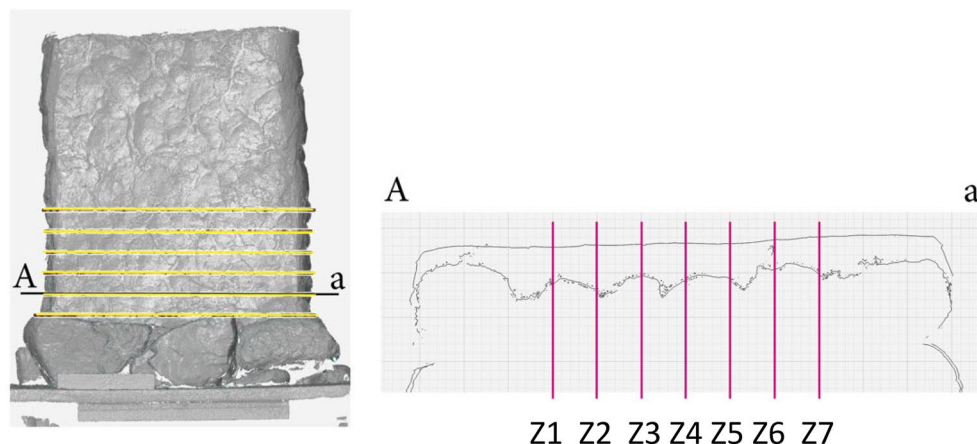


Fig. 7 Analyzing R-series walls. This shows an example from wall surface FRL. Left: Six horizontal lines for analyzation at 50 mm intervals. Right: A combined mesh of pre- and post-experiment scans, along line A-a, as seen from the bottom. Deterioration measurements from Z1 to Z7 were averaged to provide a deterioration value for the central part of the R-series wall at this height

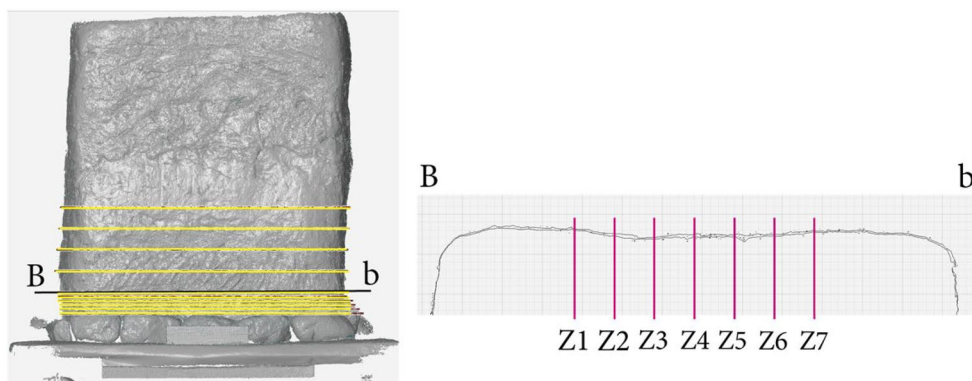


Fig. 8 Analyzing M-series walls. This shows an example from wall surface KMS1. Left: Ten examination lines were identified; six in 10 mm intervals for the bottom 51 mm, and four in 50 mm intervals above that. Right: A combined mesh of pre- and post- experiment scans, along line B-b, as seen from the bottom. Deterioration measurements from Z1 to Z7 were averaged to provide a deterioration value for the central part of the M-series wall at this height

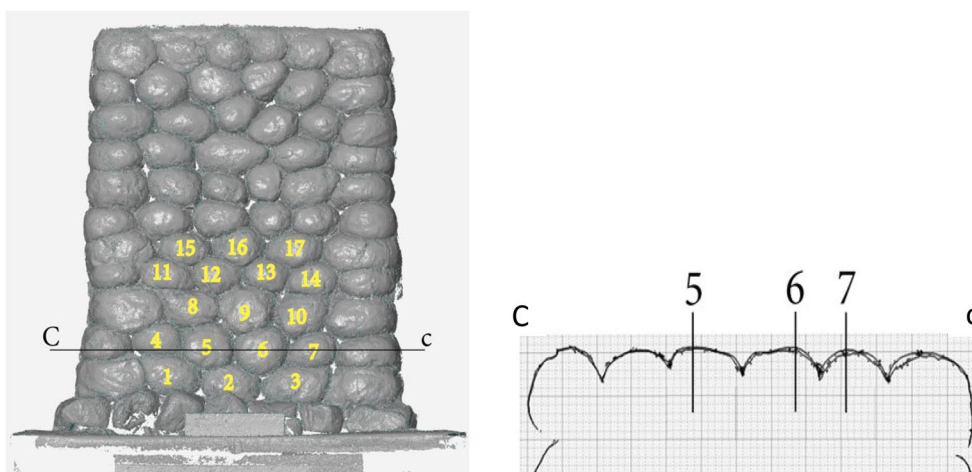


Fig. 9 Analyzing B-series walls. This shows an example from wall surface KBS. Left: balls numbered to facilitate examination. Right: A combined mesh of pre- and post- experiment scans. Deterioration was measured at the apex region of each ball. For balls 5, 6 and 7, the apex primarily occurred on the same horizontal line. Ball 4’s apex deterioration was measured from the combined mesh scans of a line slightly further up

Results

In this section, we present the visual conditions of the test wall results through scanned images, followed by graphical analysis of their deterioration.

Visible deterioration differences

Table 6 shows images of all 12 test wall surfaces prior to and following the experiment. These scans correspond to Steps 1 and 12 of Table 5. Step-1 pre-test images are in grey in Table 6, while the Step 12 blue images show the walls in a dry state after completion of all cycles of accelerated rain simulation. The test walls constructed with Kashiba earth show minimal deformity compared to those made with Fukakusa earth. Minimal surface

change is especially evident among the monolithically constructed Kashiba walls (M-series walls).

Scanned images captured before and after the test reveal significant deterioration differences among B-series walls correlating with the type of earth used. Specifically, minimal change is visible in Kashiba balls, while Fukakusa ones exhibit a notable loss of definition. R-series wall images offer a further observation; the KR-series wall surfaces exhibit well-defined cob-ball shapes even after the render has washed away, while the FR-series cob balls continue to deteriorate after the render has sloughed off. This suggests that the adhesion to the severely undulating cob-ball substrate of both “Kashiba to Kashiba” render and “Fukakusa to Fukakusa” render was poor. It also

Table 6 Before and After Scanned Images of All 12 Unstabilized Earthen Test Walls


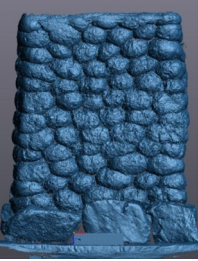

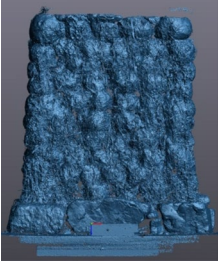

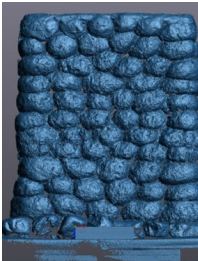

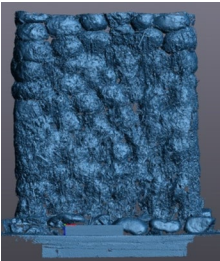
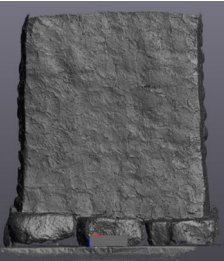


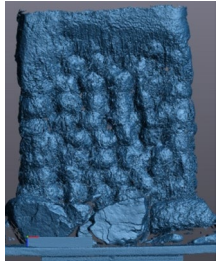
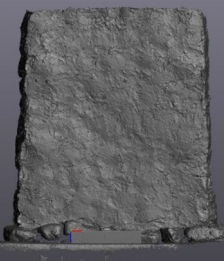
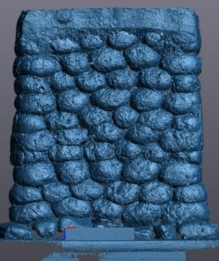
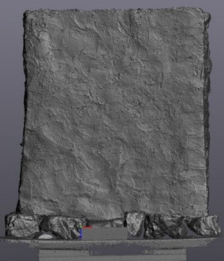
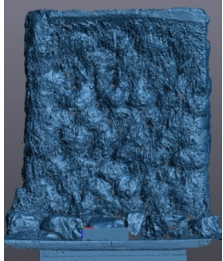

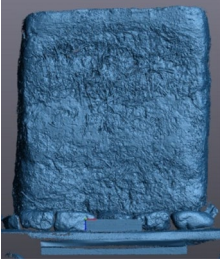

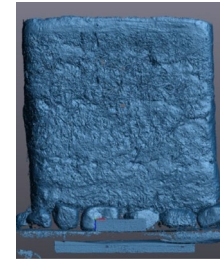
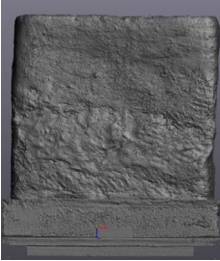
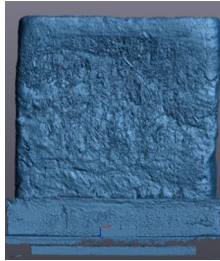
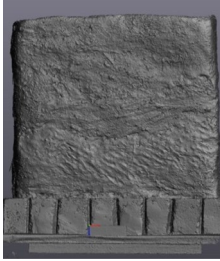
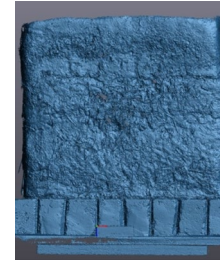
B-series			
<p>KBL before after</p>  		<p>FBL before after</p>  	
<p>KBS before after</p>  		<p>FBS before after</p>  	
R-series			
<p>KRL before after</p>  		<p>FRL before after</p>  	
<p>KRS before after</p>  		<p>FRS before after</p>  	

Table 6 (continued)

M-series			
<p>KMS1 before</p> 	<p>after</p> 	<p>KMS2 before</p> 	<p>after</p> 
<p>KMC before</p> 	<p>after</p> 	<p>KMCc before</p> 	<p>after</p> 

suggests that Kashiba earth is highly resistant to water damage, as the cob-balls mostly retain shape after the poorly adhered render falls away. This resilience is exemplified by the M-series walls, all constructed from Kashiba earth. The differences before and after 90 min of accelerated rain simulation are so subtle that they are difficult to discern with the naked eye. This highlights the value of using a 3D scanner to quantitatively measure and analyze the extent of deterioration in these wall surfaces. Table 7 shows test walls FRS, KRS, and KMC side by side as they were subjected to the accelerated rain simulation steps described in Table 5. These walls all look similar initially, but as simulated rain exposure progresses, clear differences become evident.

Comparing the stages side by side shows that Kashiba earth generally exhibits minimal deterioration. After the render washes off the KRS wall in Steps 3 and 5, there is little noticeable difference in each of the subsequent test scans. On the other hand, FRS cob balls appear less defined in every subsequent image with the exception of Steps 9 and 11, in which change is unclear. KMC stands out among the three wall types studied, exhibiting barely any visible deterioration following each testing stage.

Graphical observations

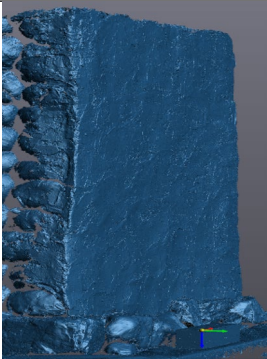
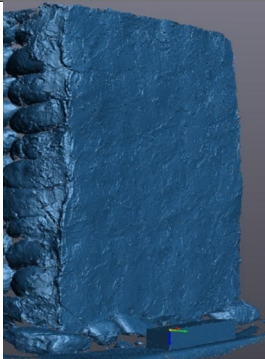
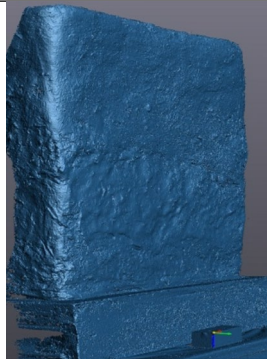
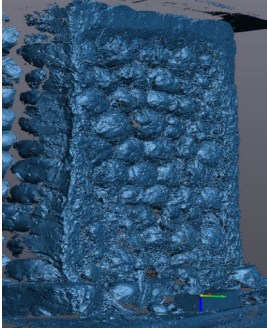
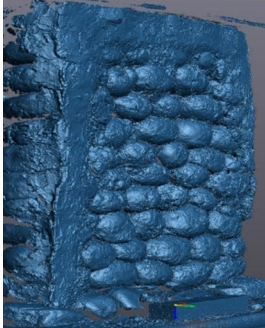
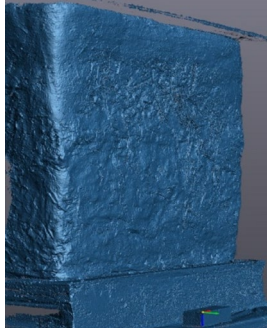
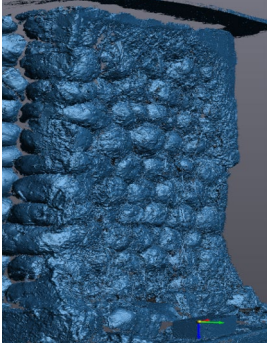
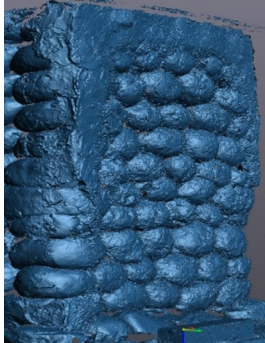
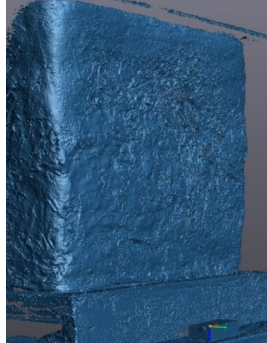
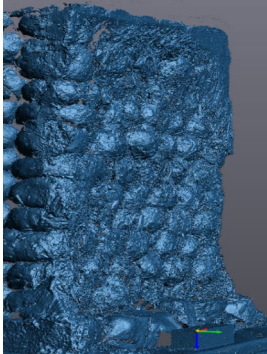
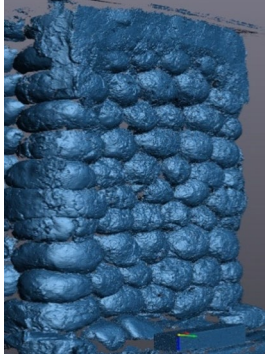

In addition to scanned images, we tracked data on changes occurring on each wall surface throughout the tests, described in the final Methods section. In the graphs below, the use of shapes and lines differentiates test wall characteristics:

- Squares represent walls made from Kashiba earth (K)
- Circles represent walls made from Fukakusa earth (F)
- ... Dotted lines represent cob-ball surface test walls (B)
- .- Dash-dot lines represent rendered test walls (R)
- Solid lines represent monolithic test walls (M)

Table 3 provides a comprehensive list of acronym definitions.

Figures 10 and 11 illustrate deterioration over time according to the steps outlined in Table 5. Dry values are greater than those after 90 min of accelerated rain exposure as water evaporates from the clay particles as the wall dries, causing the wet surface to “shrink.” These results are calculated from the central lower area of the test wall surfaces as outlined in the Methods section;

Table 7 FRS, KRS and KMC at each scanned stage

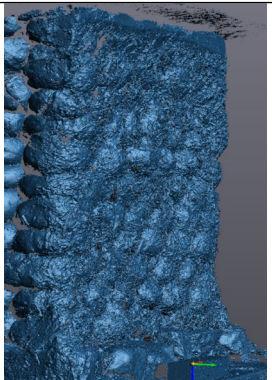
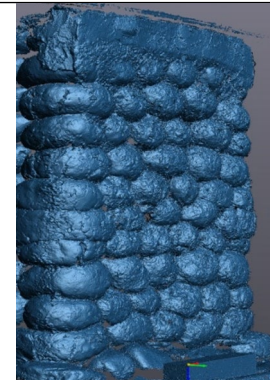
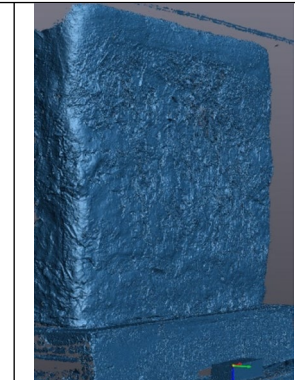
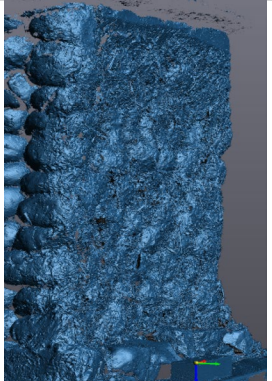
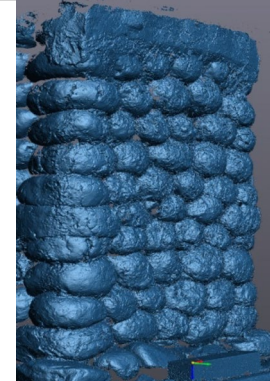
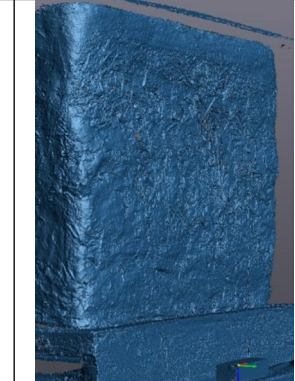
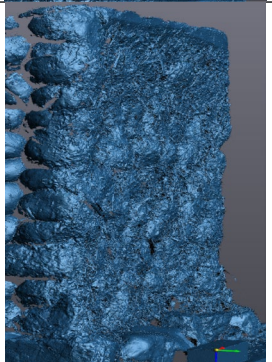
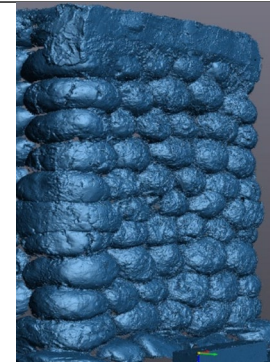
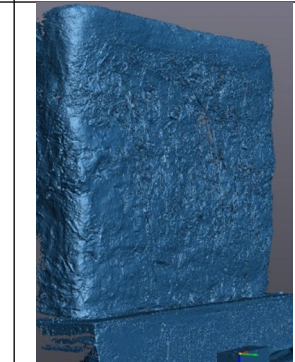
	FRS	KRS	KMC
Original wall before experiment (Step 1)			
After first 15-minute water delivery with perforated pipe (Step 3)			
After second 15-minute water delivery with central shower pattern of hose head (Step 5)			
After 30 more minutes of water delivery again with perforated pipe (Step 7)			

specifically, from the area from the foundation to a height of 250 mm, and the central 300 mm section of the test wall width.

Figure 10 contrasts B- and R-series wall deterioration. Rendered or not, walls constructed from Kashiba earth

exhibited significantly less deterioration than those of Fukakusa earth. Additionally, for both KRL and KRS, once the render sloughs off by minute 15, the deterioration line levels off, providing another indication that Kashiba earth is quite durable. Kashiba earth shrinkage

Table 7 (continued)

<p>After 15 more minutes of water delivery with lateral diffusion pattern of hose head (Step 9)</p>			
<p>After final 15 minutes of water delivery with perforated pipe (Step 11)</p>			
<p>After walls completely dry following completion of 90 minutes of accelerated rain simulation (Step 12)</p>			

in the post-test dry state is also less than that of Fukakusa earth.

Although R- and M-series walls are similar in appearance prior to testing, Fig. 10 indicates that renders in the R-series slough off too quickly, making a comparison unsuitable. Therefore, Fig. 11 compares M- and B-series walls, reinforcing the observation that the Kashiba material is highly resistant to weathering. Even simply shaped into balls, Kashiba earth deterioration after 90 min of accelerated rain simulation (6500+ mm of water exposure) is 4.7 mm for KBS and just 2.9 mm for KBL. Monolithic walls, whether on stone or concrete foundations, all deteriorated less than 4 mm (KMS1: 2.6 mm, KMS2: 3.9

mm, KMC: 1.0 mm, KMCc: 3.8 mm). The most resistant, KMC, exhibited an average deterioration of only 1 mm.

Figure 12 A-C provides side-by-side vertical cross-section analyses of each wall-type at the dry stage, illustrating deterioration patterns at various heights. In the case of B-series walls (Fig. 12 A), the ball-apexes of each of the first five layers roughly correspond to the heights indicated in the graph. Figure A, B shows a close shape resemblance in the Fukakusa and Kashiba graph lines, with each of the Ball-wall results occurring approximately 100 mm forward of the Rendered-wall results. This indicates that after the render is removed, the deterioration of the balls are consistent for both

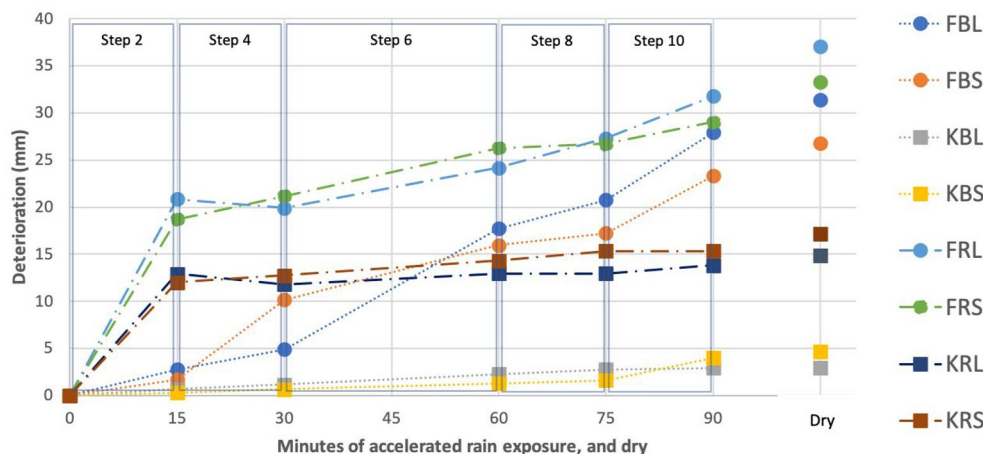


Fig. 10 Average deterioration of Ball- and Rendered-series walls at each rain simulation stage, and dry (bottom area from foundation to 250 mm in height)

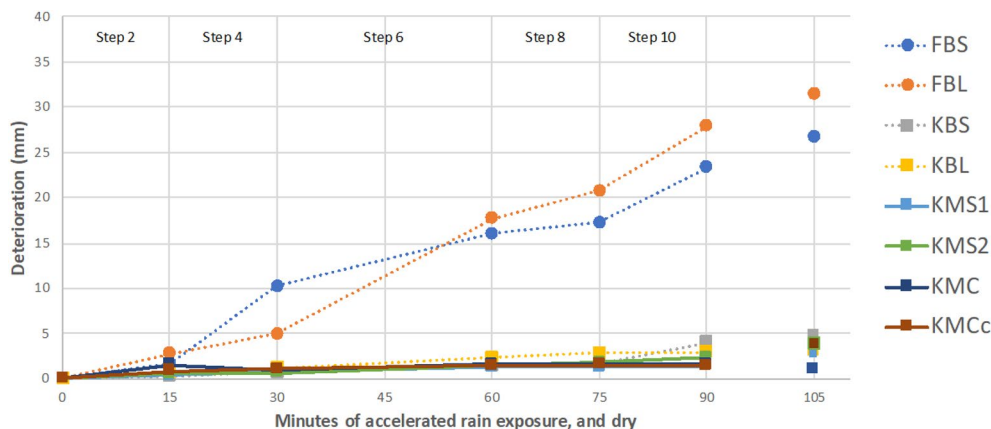


Fig. 11 Average deterioration of Monolithic- and Ball-series at each rain simulation stage, and dry (bottom area from foundation to 250 mm in height)

Fukakusa and Kashiba earths. Figure 12 C shows again that minimal surface erosion occurred with Kashiba earth monolithic walls.

Interestingly, viewed like this in Figure 12 A-C, the vertical cross-section reveals a pattern in the shape of each graph line, manifesting as a reverse "S" shape. This observation will be explored in Discussion.

Discussion

We performed accelerated “rain” tests on two types of walls (cob-ball and monolithic cob) built using two locally-used earthen construction materials (Fukakusa and Kashiba), and measured results throughout the duration of these 90-min tests using a 3D scanner.

The following data and insights were gained from our experiment.

Need for further investigation of foundation types

The differences in deterioration observed in walls with small and large stone foundations are inconclusive. As is visible from Fig. 10, Kashiba earth displays less deterioration with large stone foundations, while Fukakusa earth shows less deterioration with small stone foundations.

Examining the results depicted in Fig. 11 at the dry stage, we did not observe any correlation between test wall surface deterioration and foundation characteristics. Fukakusa walls were already discussed in the previous paragraph. When considering only the Kashiba walls of Fig. 11, deterioration ranged from least to most pronounced as follows: KMC, KMS1, KBL, KMCc/

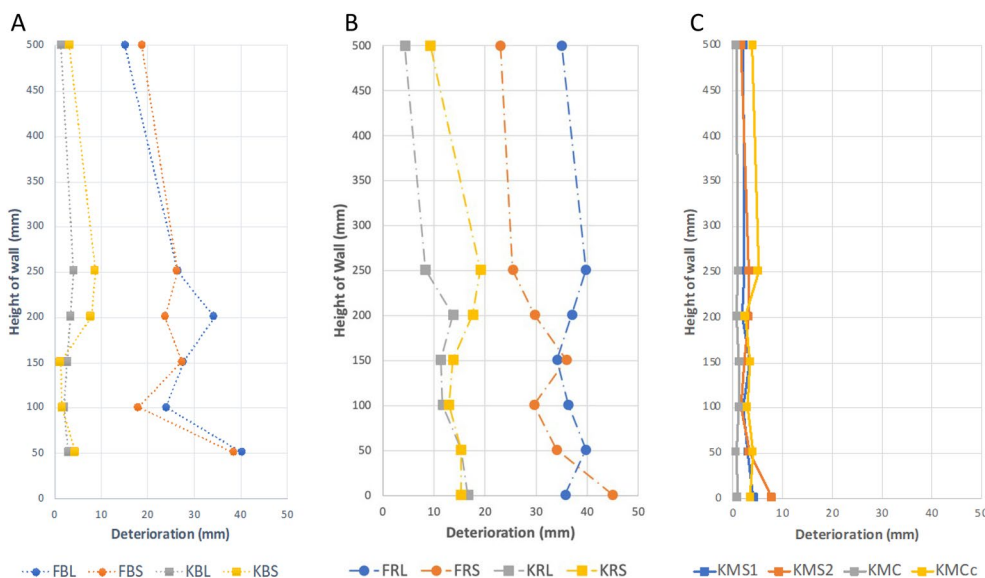


Fig. 12 Vertical cross-section analysis of wall surfaces illustrating deterioration patterns at all heights of the test wall, at dry stage. **A** Average deterioration of Ball-series wall surfaces. **B** Average deterioration of Render-series wall surfaces. **C** Average deterioration of Monolithic-series wall surfaces

KMS2 (statistically equivalent), and finally KBS. However, extracting a clear pattern from these results is challenging.

It may be that different compositions of earth materials lead to different deterioration behaviors, suggesting that some earths may exhibit greater structural stability when used for continuous foundations, while others may perform better in scenarios where the foundation has breaks to channel water away. Further research is imperative to establish more robust conclusions in this regard.

The value of practitioner knowledge

Of the two types of earth used in our experiment, Kashiba is the type which is traditionally used as a primary component forming the bulk of earthen walls—the base layer. It serves to provide substance and strength to the walls. In contrast, layers applied over it, such as Fukakusa-earth-based plasters and renders, act as cosmetic enhancement, bringing out the aesthetic qualities of the walls. While we were aware of this at the onset of the experiment, we were surprised at just how well Kashiba earth performed. After 90 min of accelerated rain simulation totaling over 6500 mm of water exposure, the six Kashiba Ball- and Monolithic-wall surfaces all showed an average of less than 5 mm erosion, with the most resistant averaging only 1 mm.

Based on the duration and amount of water exposure in our experiment, we tentatively estimate that the test walls underwent an equivalent of four years of Kyoto rainfall, given the city’s average annual rainfall is approximately

1677 mm [30]. It is crucial to acknowledge the limitations in our work as our test did not include wet-dry cycles, freeze–thaw cycles, or variations in rainfall direction and intensity due to wind. Yet, our conjecture gains significance when compared to the results of Bui et. al. [23]. Although Bui et al.’s study focused on rammed earth (RE), Chabriac et al. [34] note that certain inherent properties of earth materials can establish correlations across different building types, despite variations in construction techniques. They suggest that, as both cob and RE involve stacked layers of soil, their liquid saturation limits would be highly similar [34].

Bui et al.’s 2009 investigation centered on RE exposed to 20 years of outdoor natural weathering in a French alpine valley with an annual precipitation of approximately 1000 mm. Similar to the material sourcing of our experiment, materials were specifically obtained from a region with an RE building tradition. Their unstabilized RE wall experienced erosion of 6.4 mm over a 20-year period. This led to the conclusion that the damage was purely aesthetic, indicating that structural integrity was not compromised. It also suggests potential stability for up to 60 years [23]. In a thought experiment, if our walls were exposed to an equivalent of four years of rain exposure in Kyoto, and erosion of KMC averaged 1 mm, then it may be that the KMC test wall surface would experience 5 mm erosion over the course of 20 years. This is close to Bui et al.’s findings for the RE wall with 6.4 mm erosion. It would be interesting to build a test wall to expose to

the natural elements in Kyoto for a 20-year period with Kashiba earth and confirm this hypothesis.

In sum, our findings instill confidence in the durability of the materials used when sourced according to regional professional knowledge. This expertise stands as a valuable asset, and can elevate research endeavors aimed at creating optimal, environmentally responsible architecture.

“Added material” phenomenon

The reverse “S” curves seen in Fig. 12A, B and C of the Results section above parallels an observation made by Richards et al. [10]. Through post-test 3D scans, they found that parts of their sample wall exposed to weathering tests had areas with “added material.” We can imagine that as precipitation erodes unstabilized earth, gravity pulls it towards the ground and uneven wall surfaces may “catch and hold” the traveling particles. Or, traveling particles may simply not make it to the ground before the rain stops, and the material dries in place. In these ways, material can stop, dry and ultimately become “added” to its new location. If clay particles are uncoated (unstabilized), their sticky nature may also be a factor of this observed phenomenon.

In each of our Fig. 12A–C, the upper tested area of the wall displays erosion, accompanied by a noticeable bulge further down, followed by additional erosion at the base. It is possible that the eroded material in the lowest part of the wall washes off completely, while particles higher up accumulate in a “stop and add” manner further along down the bottom portion. Investigating the consistency of this pattern across earthen structures would potentially provide valuable insights into the behavior of unstabilized earthen materials. This exploration could inform best practices for construction and contribute to a deeper understanding of the durability factors affecting earthen structures. If the observed pattern proves consistent, it would be interesting to explore whether the “added material” phenomenon contributes to the longevity observed in many extant earthen structures.

Wall maintenance

Damage is sustained by earthen walls through multiple avenues. Weathering causes damage over time. Our experiment accelerated this phenomenon and the results provided visual and graphical data to quantify the damage caused by water. Rendered cob-ball wall surfaces, particularly those made with the resilient Kashiba earth, showed the surface render fail and wash off, while the base layer underneath sustained damage much more slowly.

Not only is the damage repairable, but this maintainability is unique to unstabilized earthen walls in particular. In fact, while researching repair mortars for heritage site RE walls, Gomes et al. [3] found that unstabilized materials were the most effective for patching damaged areas.

Where a culture of maintenance for vernacular earthen architecture exists, we can learn what local heritage craftspersons do to maintain structures. In Kyoto, fourth-generation plasterer Sato Hiroyuki explains: “Exterior finish plasters typically have a lifespan of 20 to 50 years, after which they may require surface removal and reapplication. After 150 years, the base layer of the structure often shows damage that necessitates more extensive repairs” [personal communication, July 26, 2022]. These observations underscore the repairability of earthen materials and suggest suitable considerations when planning construction with earth.

Umubyeyi et al.’s 2023 study [22] of a large unstabilized RE test wall concluded that after 16 years, conservative calculations for erosion by weathering in highly exposed sections was 3.5 mm/year; medium level exposure erosion rate was 1.5 mm/year; and areas with low levels of exposure eroded at a rate of 0.5 mm/year. To maintain structural viability on a 300 mm thick RE wall, it would take at least 37 years before repairs would be required on highly exposed areas, and at most 75 years for areas of medium exposure.

With maintenance, an unstabilized earthen structure’s anticipated lifespan can extend across centuries.

Hose test

Put simply, one could liken our experiment to a glorified hose test, where we used refined technology to take durability measurements after turning a hose onto unstabilized earthen walls. The equipment used for our accelerated rain simulation test consisted of a hose, a showerhead, and a narrow pipe perforated with many holes. We consistently monitored the water flow rate with a water flow meter, an inexpensive online purchase. Our simple equipment is in sharp contrast to more complex testing systems such as one designed by Ogunye and Boussabaine [19], and the climatic chamber used by Arrigoni et al. [9]. Using simple, easily accessible tools, we could clearly differentiate between a good earthen material for building versus one not suited for structural purposes. This was clear even before measurements were taken, as evidenced in Tables 6 and 7.

Our results suggest that hose-and-showerhead durability tests could be adequate for identifying acceptable levels of erosion of unstabilized earthen materials. Such tests could also be used for materials

containing stabilizers and could meet the need for a standard, repeatable durability test across all materials.

The challenge will be in identifying acceptable erosion. An international effort to achieve consensus would be most beneficial. Testing vernacularly used building-grade earths worldwide, measuring their deterioration with various showerhead settings and water flow volumes, would provide valuable insights. The data could be collected, combined and analyzed to learn if a common erosion rate could be identified. Since we know that minute erosion is not a safety issue, and that earthen walls are repairable/replasterable, then theoretically, limits for acceptable erosion could be established.

While water pressure/volume, fall distance, and impact angle are important variables requiring control, we propose a simple test and classification parameter. This would involve identifying a common, universal setting on standard hose showerhead attachments, equipped with a water flow meter for volumetric measurements. Such meters are easily attainable and simple to connect, unlike equipment for pressure measurements. With this simple equipment, a formula for standards could be identified. The following example uses a blank space and capital alphabets to provide text for what such a standard may look like:

Set the shower head to a “()” setting. With a water flow volume greater than (A) liters per minute and less than (B) liters per minute, place the nozzle of the showerhead (a distance of C) away from and (a distance of D) above the target area. Continuously spray the test wall for (E amount of time). If erosion of the target area is less than (E) mm on average, the material is adequate.

This proposed type of standard test uses commonly accessible tools and can help earthen wall builders with material selection. Methods for test sample construction will also need to be identified. At building sites, in-situ tests could be conducted on sample walls constructed using methods identical to those to be used in the actual construction, demonstrating potential outcomes for the proposed building.

Millimeter-level measurements can be achieved without a 3D scanner. Umubyeyi et al. used a plumb line and a caliper for their measurements [22]. A simple plumb line and caliper could be used for standard measurements in this way.

It may be that the value of a hose-showerhead erosion test lies in its simplicity. In selecting a use-appropriate material, builders of past generations analyzed earthen materials by observing how they behaved. Similarly, in determining building-grade earth durability today, the “hose test” may provide the information required to

make informed decisions on material selection, ensuring the longevity and resilience of earthen structures.

Conclusion

Our tests measured fundamental durability characteristics of unstabilized earth using accelerated rain simulation on variously built cob walls. Deterioration measurements with 0.1 mm accuracy were obtained through 3D scanning. Analysis was based on 6500 mm of “rain” exposure over the course of 90 min, falling from three meters in height, with defined volumes implemented by different shower settings. The material favored locally by vernacular craftspeople for the core earthen substrate eroded least. Tested as a monolithic cob construction on four unique foundation scenarios, erosion measured 1 mm, 2.6 mm, 3.8 mm and 3.9 mm respectively, suggesting the viability of this material in construction.

- We confirmed our hypothesis that unstabilized earth is a viable option for construction material in terms of weather resilience.
- It is recommended that quantifying vernacular methodology be advanced as an academic field. This could expedite successful transitions to architecture comprising environmentally friendly, durable and maintainable earthen materials.
- Hose-and-showerhead tests can prove useful to inform material durability. An internationally acceptable standard could be developed using only this equipment. Such a test could work on stabilized and unstabilized earthen materials alike.

In conclusion, the use of unstabilized earthen building materials aligns with United Nations Sustainable Development Goals and other environmental demands. We have described a case in which the identification of earthen building materials by local expertise in Japan corresponds with the requirement for durable, use-appropriate unstabilized earthen walls.

Future research in Japan should prioritize exploring existing techniques which improve durability and workability of earthen material, such as exploring the fermentation—for over several months to two years—of a core-layer earthen material/chopped straw mixture. Further exploration of methods from various cultures is indicated.

Abbreviations

EBC	Earth-based construction
FBL	Fukakusa-earth ball wall on large stone foundation
FBS	Fukakusa-earth ball wall on small stone foundation
FRL	Fukakusa-earth rendered wall on large stone foundation
FRS	Fukakusa-earth rendered wall on small stone foundation
KBL	Kashiba-earth ball wall on large stone foundation

KBS	Kashiba-earth ball wall on small stone foundation
KMC	Kashiba-earth monolithic wall on concrete foundation
KMCc	Kashiba-earth monolithic wall on concrete foundation with vertical channels
KMS1	Kashiba-earth monolithic wall on foundation of five small stones
KMS2	Kashiba-earth monolithic wall on foundation of six small stones
KRL	Kashiba-earth rendered wall on large stone foundation
KRS	Kashiba-earth rendered wall on small stone foundation
RE	Rammed earth

Acknowledgements

The authors would like to thank Professor Wataru Nakamura, Senior Lecturer, Faculty of Engineering Department of Innovative Engineering, Division of Architecture and Civil Engineering, Ashikaga University for performing the particle distribution analysis of the Kashiba earth. The authors would also like to acknowledge Wanda Miyata for editing the paper, as well as Chris Irwin who did a final readability/grammar check. We would also like to thank the technicians of the Advanced Technology Center of Kyoto Institute of Technology, Mr. Koyama and Mr. Shikata, for their assistance in building the testing room. In addition, we would like to thank the undergraduate students who assisted with building the cob ball walls.

Author contributions

Both authors developed the design for the experiment. EKR built the test walls, performed the scans, and analyzed the data. MM guided the analysis and presentation of results in the manuscript, which was written by EKR. Both authors read and approved the final manuscript.

Funding

The authors received no funding for the research conducted for this paper.

Availability of data and materials

The datasets generated and/or analysed during the current study are not publicly available due being property of Kyoto Institute of Technology but are available from the corresponding author on reasonable request. The intellectual property rights of the Point Cloud Data (Fig. 4, Fig. 7, Fig. 8, Fig. 9, Table 6, Table 7) used in this article belong to the Kyoto Institute of Technology. Should you wish to use them, please contact at dpoint@kit.ac.jp.

Declarations

Ethics approval and consent to participate

Not applicable.

Competing interests

The authors declare no competing interests.

Received: 22 December 2023 Accepted: 19 April 2024

Published online: 14 May 2024

References

- Van Damme H, Houben H. Earth concrete. Stabilization revisited. *Cem Concr Res*. 2018;114:90–102. <https://doi.org/10.1016/j.cemconres.2017.02.035>.
- Losini AE, Grillet AC, Bellotto M, Woloszyn M, Dotelli G. Natural additives and biopolymers for raw earth construction stabilization—a review. *Constr Build Mater*. 2021;304: 124507. <https://doi.org/10.1016/j.conbuildmat.2021.124507>.
- Gomes MI, Faria P, Goncalves TD. Rammed earth walls repair by earth-based mortars: the adequacy to assess effectiveness. *Constr Build Mater*. 2019;205:213–31. <https://doi.org/10.1016/j.conbuildmat.2019.01.222>.
- Danso H, Martinson B, Ali M, Mant C. Performance characteristics of enhanced soil blocks: a quantitative review. *Build Res Inf*. 2014;43(2):253–62. <https://doi.org/10.1080/09613218.2014.933293>.
- Morel JC, Charef R. What are the barriers affecting the use of earth as a modern construction material in the context of circular economy? *IOF Conf Ser Earth Environ Sci*. 2019;225: 012053. <https://doi.org/10.1088/1755-1315/225/1/012053>.
- Raj A, Sharma T, Singh S, Sharma U, et al. Building a sustainable future from theory to practice: a comprehensive PRISMA-guided assessment of compressed stabilized earth blocks (CSEB) for construction applications. *Sustainability*. 2023;15:9374. <https://doi.org/10.3390/su15129374>.
- Beckett CTS, Jaquin PA, Morel JC. Weathering the storm: a framework to assess the resistance of earthen structures to water damage. *Constr Build Mater*. 2020;242: 118098. <https://doi.org/10.1016/j.conbuildmat.2020.118098>.
- Medvey B, Dobszay G. Durability of stabilized earthen constructions: a review. *Geotech Geol Eng*. 2020;38:2403–25. <https://doi.org/10.1007/s10706-020-01208-6>.
- Arrigoni A, Grillet AC, Pelosato R, Dotelli G, et al. Reduction of rammed earth's hygroscopic performance under stabilization: an experimental investigation. *Build Environ*. 2017;115:358–67. <https://doi.org/10.1016/j.buildenv.2017.01.034>.
- Richards J, Zhao G, Zhang H, Viles H. A controlled field experiment to investigate the deterioration of earthen heritage by wind and rain. *Heritage Science*. 2019;7:51. <https://doi.org/10.1186/s40494-019-0293-7>.
- Seco A, Urmeneta P, Prieto E, Marcelino S, et al. Estimated and real durability of unfired clay bricks: Determining factors and representativeness of the laboratory tests. *Constr Build Mater*. 2017;131:600–5. <https://doi.org/10.1016/j.conbuildmat.2016.11.107>.
- Guettala A, Abibsi A, Houari H. Durability study of stabilized earth concrete under both laboratory and climatic conditions exposure. *Constr Build Mater*. 2006;20(3):119–27. <https://doi.org/10.1016/j.conbuildmat.2005.02.001>.
- Beckett C, Faria P. Defining a generic accelerated erosion testing method for earthen materials. *E3S Web of Conf*. 2023;382:05002. <https://doi.org/10.1051/e3sconf/202338205002>.
- Hamard E, Cazacliu B, Razakamanantsoa A, Morel J-C. Cob, a vernacular earth construction process in the context of modern sustainable building. *Build Environ*. 2016;106:103–19. <https://doi.org/10.1016/j.buildenv.2016.06.009>.
- Reynolds EK, Muramoto M. Circumstances contributing to the deterioration of old cob structures in Japan. *J Asian Arch Build Eng*. 2022;21(5):1980–2008. <https://doi.org/10.1080/13467581.2021.1967755>.
- Hatanaka K, Muramoto M, Yamada M, Nakamura W. Mud and stone masonry construction method in Japan - Report 4 Research on building use of hanya in Tanba Sasayama. *Summaries of Technical Papers of Annual Meeting, Architectural planning and design, AIJ*. (in Japanese) 2020;1279–1280.
- Nakamura W, Yamada M, Muramoto M, Hatanaka K. Mud and stone masonry construction method in Japan report 1: The measurement of the warehouses and the walls in Yamonobenomichi, Nara Prefecture. *Journal of Technology and Design, AIJ*. (in Japanese) 2019;25(60):875–880. <https://doi.org/10.3130/aijt.25.875>.
- Hall MR. Assessing the environmental performance of stabilized rammed earth walls using a climatic simulation chamber. *Build Environ*. 2007;42(1):139–45.
- Ogunye FO, Boussabaine H. Development of a rainfall test rig as an aid in soil block weathering assessment. *Constr Build Mater*. 2002;16(3):173–80. [https://doi.org/10.1016/S0950-0618\(02\)00010-7](https://doi.org/10.1016/S0950-0618(02)00010-7).
- Luo Y, Yang M, Ni P, Peng X, et al. Degradation of rammed earth under wind-driven rain: the case of Fujian Tulou, China. *Constr Build Mater*. 2020;261:119989. <https://doi.org/10.1016/j.conbuildmat.2020.119989>.
- Hart S, Raymond K, Williams CJ, Johnson J, et al. Precipitation impacts on earthen architecture for better implementation of cultural resource management in the US Southwest. *Herit Sci*. 2021;9:143. <https://doi.org/10.1186/s40494-021-00615-z>.
- Umubyeyi C, Wenger K, Dahmen J, Ochsendorf J. Durability of unstabilized rammed earth in temperate climates: a long term study. *Constr Build Mater*. 2023;409(5): 133953. <https://doi.org/10.1016/j.conbuildmat.2023.133953>.
- Bui QB, Morel JC, Venkatarama Reddy BV, Ghayad W. Durability of rammed earth walls exposed for 20 years to natural weathering. *Build Environ*. 2009;44(5):912–9. <https://doi.org/10.1016/j.buildenv.2008.07.001>.

24. Millogo Y, Aubert JE, Sere AD, Fabbri A, et al. Earth Blocks stabilized by cow-dung. *Mater Struct*. 2016;49:4583–94. <https://doi.org/10.1617/s11527-016-0808-6>.
25. Koshiishi N, Inden T. Properties of wall clays in main districts: Wall clays for clay wall on bamboo lathing Part 1. *Journal of Structural and Construction Engineering, AIJ*. (in Japanese) 2008;73(631)1467–1474. <https://doi.org/10.3130/aijs.73.1467>
26. A&D MX-50 Moisture Analyzer, https://weighing.andonline.com/product/moisture-analyzers/mx-50?commerce_product=37. Accessed 9 Mar 2024
27. Hatanaka K, Kimura H, Makoto M, Kato A. The examination of traditional construction method of mud wall: a study on construction characteristics of Cob-wall through experimental construction. *design research*. (in Japanese) 2016;72:113–20. https://doi.org/10.24520/designresearch.72.0_113.
28. Liloia Z. How to Mix the Perfect Batch of Cob. *The Year of Mud blog*. 2015. <https://theyearofmud.com/2015/02/16/building-with-cob-how-to-mix/>. Accessed 15 Aug 2021
29. Nielsen KT, Moldrup P, Thorndahl S, et al. Automated rainfall simulator for variable rainfall on urban green areas. *Lakes Reserv*. 2019;33(26):3364–77. <https://doi.org/10.1002/hyp.13563>.
30. "Average monthly snow and rainfall in Kyoto (Kyoto) in inches." *Weather-and-Climate*. 2023. <https://weather-and-climate.com/average-monthly-precipitation-Rainfall-inches,kyoto,Japan>. Accessed 8 Feb 2023
31. Creaform GoSCAN 3D 50 G2 SCANNER, <https://www.creaform3d.com/en/goscan-3d-g2-scanner>. Accessed 12 Mar 2024
32. VXelements, <https://www.creaform3d.com/en/metrology-solutions/3d-applications-software-platforms/vxmodel-scan-cad-software-module>. Accessed 23 Jun 2023
33. GOM Inspect, <https://www.gom.com/en/products/zeiss-quality-suite/gom-inspect-pro> Accessed 30 Jun 2023
34. Chabriac PA, Fabbri A, Morel JC, Laurent JP, et al. A procedure to measure the in-situ hygrothermal behavior of earth walls. *Materials*. 2014;7:3002–20. <https://doi.org/10.3390/ma7043002>.
35. Zhang X, Nowamooz H. Effect of rising damp in unstabilized rammed earth (URE) walls. *Constr Build Mater*. 2021;307: 124989. <https://doi.org/10.1016/j.conbuildmat.2021.124989>.
36. Luo Y, Zhou P, Ni P, Peng X, Ye J. Degredation of rammed earth under soluble salts attack and drying-wetting cycles: The case of Fujian Tulou. *China Applied Clay Science*. 2021;212: 106202. <https://doi.org/10.1016/j.clay.2021.106202>.

Publisher's Note

Springer Nature remains neutral with regard to jurisdictional claims in published maps and institutional affiliations.